OPEN ACCESS
CellPress

Cell Reports
Article

A Humanized Mouse Identifies the Bone Marrow as a Niche with Low Therapeutic IgG Activity

Anja Lux,[1] Michaela Seeling,[1] Anne Baerenwaldt,[1] Birgit Lehmann,[1] Inessa Schwab,[1] Roland Repp,[2] Norbert Meidenbauer,[3] Andreas Mackensen,[3] Arndt Hartmann,[4] Gordon Heidkamp,[5] Diana Dudziak,[5] and Falk Nimmerjahn[1,*]

[1]Institute of Genetics, Department of Biology, University of Erlangen-Nürnberg, Erwin-Rommelstrasse 3, 91058 Erlangen, Germany
[2]Medical Department V, Klinikum am Bruderwald, Bugerstrasse 80, 96049 Bamberg, Germany
[3]Department of Internal Medicine 5-Hematology/Oncology, University Hospital of Erlangen, Ulmenweg 18, 91054 Erlangen, Germany
[4]Department of Pathology, University Hospital of Erlangen, Krankenhausstrasse 8, 91054 Erlangen, Germany
[5]Department of Dermatology, University Hospital of Erlangen, Hartmannstrasse 14, 91052 Erlangen, Germany
*Correspondence: falk.nimmerjahn@fau.de
http://dx.doi.org/10.1016/j.celrep.2014.02.041

SUMMARY

Genetic differences between humans and in vivo model systems, including mice and nonhuman primates, make it difficult to predict the efficacy of immunoglobulin G (IgG) activity in humans and understand the molecular and cellular mechanisms underlying that activity. To bridge this gap, we established a small-animal model system that allowed us to study human IgG effector functions in the context of an intact human immune system without the interference of murine Fcγ receptors expressed on mouse innate immune effector cells in vivo. Using a model of B cell depletion with different human IgG variants that recognize CD20, we show that this humanized mouse model can provide unique insights into the mechanism of human IgG activity in vivo. Importantly, these studies identify the bone marrow as a niche with low therapeutic IgG activity.

INTRODUCTION

The therapeutic success of immunoglobulin G (IgG) antibodies such as rituximab (a chimeric CD20-specific IgG1 antibody) and herceptin (a her2/neu-specific IgG1 antibody) in the treatment of human cancer and autoimmune disease has fueled interest in the widespread development of IgG-based biologicals (Carter, 2006; St Clair, 2009; Waldmann, 2003; Weiner et al., 2010). Animal model systems frequently used for the preclinical evaluation of IgG activity and safety include mice, rats, and a variety of nonhuman primate species. Because they provide the possibility to delete genes of choice, mouse in vivo model systems are widely used, and many of our current models of IgG activity stem from data obtained in mice. Indeed, such studies have provided valuable insights into the mechanism of IgG activity, such as the importance of cellular Fcγ receptors (FcγR) for IgG activity and the role of individual FcγRs in IgG subclass activity in vivo (Beers et al., 2008; Hogarth, 2002; Nimmerjahn and Ravetch, 2008; Takai, 2002). The relevance of these basic studies to the human system is supported by data showing that cancer patients respond better to anticancer antibodies if they express allelic variants of FcγRs that confer enhanced binding to the IgG subclass of the therapeutic antibody (Cartron et al., 2002; Musolino et al., 2008; Weng et al., 2004; Weng and Levy, 2003). Despite the similarities between mice and humans, however, there are several important differences, such as the cell-type-specific expression pattern of certain FcγRs and the capacity of some mouse FcγRs to interact with other Ig isotypes, which are not reflected in humans (Hirano et al., 2007; Lux and Nimmerjahn, 2013; Mancardi et al., 2008; Nimmerjahn et al., 2010; Biburger and Nimmerjahn, 2012). As mentioned in previous studies, allelic variants of the low-affinity FcγRs FcγRIIB, FcγRIIA, and FcγRIIIA are present in the human population that can impact either the affinity or functionality of these receptors (Baerenwaldt et al., 2011; Bruhns et al., 2009; Lux et al., 2013; Smith and Clatworthy, 2010). Moreover, certain human FcγRs, such as the neutrophil-specific FcγRIIIB, are not present in mice at all. Thus, several factors that potentially influence IgG activity in humans are not recapitulated in any of the currently available animal models, including nonhuman primates. To combine the advantages of a small-animal model with the possibility to study the human immune system in vivo, we used the Rag2/*Il2rg*-deficient mouse strain (Rag2/γc−/−), in which a functional human immune system can develop upon injection with purified human hematopoietic stem cells (HSCs) due to the absence of mouse B cells, T cells, and functional natural killer (NK) cells (Legrand et al., 2008; Shultz et al., 2012;Traggiai et al., 2004; Legrand et al., 2009). Although these mice are an excellent model system for studying the development of the human immune system, they may not be the optimal system for studying human IgG activity in vivo. This is due to the presence of mouse monocytes, macrophages, and neutrophils expressing high levels of mouse activating FcγRs, which have the capacity to interact with human IgG1 antibodies (Lux and Nimmerjahn, 2013). Further complicating the situation, the absence of mouse B cells and mouse serum antibodies will result in a high capacity of the mouse high-affinity FcγRI, which is usually

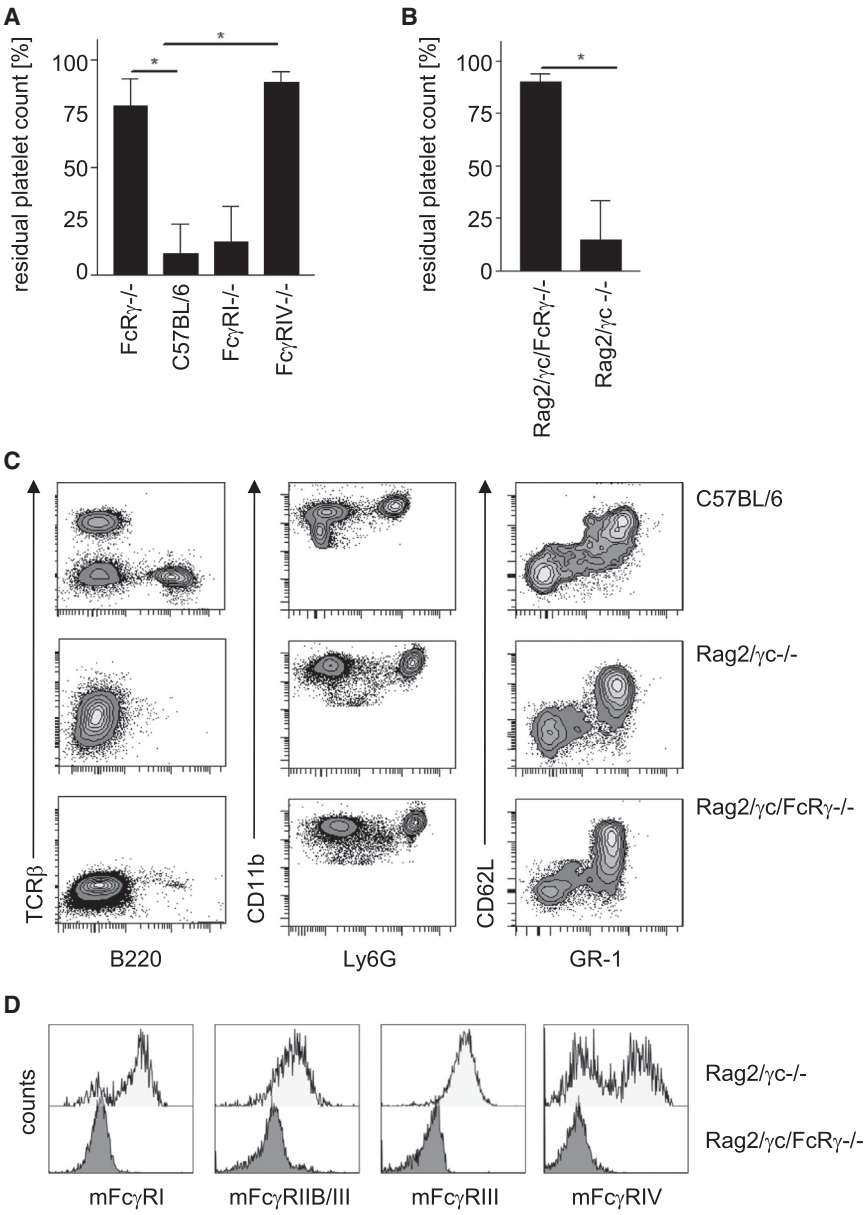

Figure 1. Generation and Characterization of Rag2/γc/FcRγ Knockout Mice

(A and B) Residual platelet counts in the peripheral blood of FcRγ-, C57BL/6, FcγRI−/−, and FcγRIV−/− mice (A) or Rag2/γc−/− and Rag2/γc/FcRγ−/− mice (B) upon injection of the humanized antiplatelet 6A6-hIgG1 antibody.

(C) Analysis of PBMCs in C57BL/6, Rag2/γc−/−, and Rag2/γc/FcRγ−/− mice by flow cytometry, identifying mouse T (TCRβ), B (B220), neutrophil (CD11B+ and Ly6G+), and Ly6C+ and Ly6C− (GR-1) monocyte subsets.

(D) Expression of the indicated murine FcγRs on CD11b+ PBMCs of Rag2/γc−/− and Rag2/γc/FcRγ−/− mice. Bar graphs indicate mean residual platelet counts ± SD of at least two independent experiments with three to five mice each. Statistical analysis was performed by Mann-Whitney test. Asterisks indicate values with a significant difference; *$p < 0.05$.

RESULTS

Generation and Characterization of Rag2/γc/FcRγ−/− Mice

Although Rag2/γc−/− mice have allowed unique insights into human immune system development and function to be obtained, studying human IgG activity in this and other immunodeficient mouse strains transplanted with human peripheral blood mononuclear cells (PBMCs) are hampered by the fact that many human IgG subclasses, and especially human IgG1, which is the most abundant IgG subclass used in human therapy, can bind to mouse activating FcγRI and FcγRIV (Lux and Nimmerjahn, 2013). To test whether human IgG1 can indeed mediate its activity via one of these mouse FcγRs in vivo, we generated a humanized IgG1 variant of the mouse platelet-specific antibody 6A6 (Nimmerjahn et al., 2005; Nimmerjahn and Ravetch, 2005). Indeed, 6A6-hIgG1 efficiently depleted platelets in C57BL/6 and FcγRI-deficient mice, but was not able to remove platelets in FcRγ-deficient mice lacking all activating FcγRs and in FcγRIV-deficient animals, consistent with previous studies that demonstrated an important role for this mouse activating FcγR in IgG activity in vivo (Figures 1A and 1B; Nimmerjahn et al., 2005, 2010; Seeling et al., 2013; Biburger et al., 2011; Mancardi et al., 2011; Otten et al., 2008; Kasperkiewicz et al., 2012; Syed et al., 2009; Baudino et al., 2008; Kaneko et al., 2006; Hamaguchi et al., 2006). These results emphasize that studying human IgG activity in currently available immunodeficient mouse strains transplanted with human immune cells will not allow us to distinguish between effector functions mediated by mouse and human innate immune effector cells unless we can discover transplantation conditions that occupied with mouse serum IgG2a, to interact with human IgG1, thereby artificially skewing antibody effector functions toward this receptor.

Thus, we set out to generate an immunodeficient mouse model that would accept human HSC grafts without expressing mouse activating FcγRs. We show that this mouse strain efficiently accepts human HSC grafts, which develop into a human immune system containing all the major hematopoietic cell lineages. By using human CD20-specific monoclonal antibodies, we demonstrate that human IgG subclasses have a differential activity in vivo and depend critically on the IgG constant fragment. Moreover, this model system allowed us to identify physiological niches, such as the bone marrow, in which human IgG activity might be less effective.

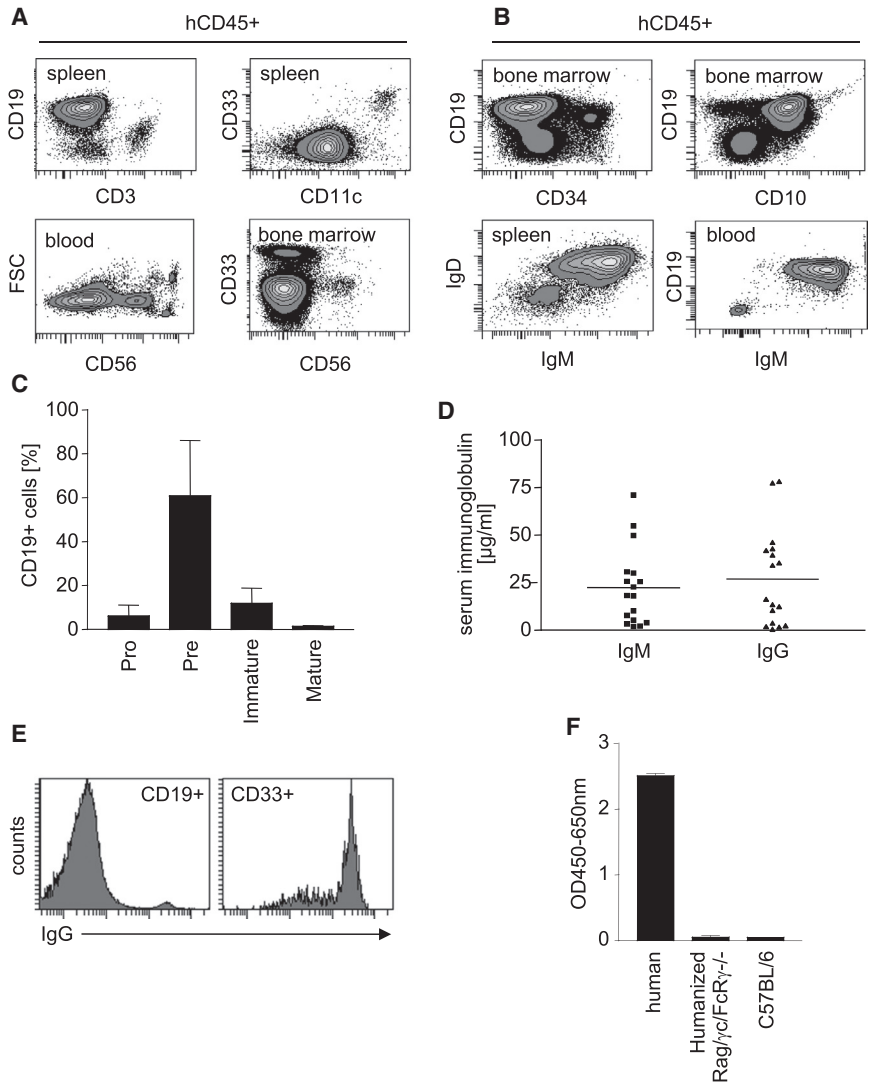

Figure 2. Characterization of Human Immune System Development in Rag2/γc/FcRγ−/− Mice

(A) Identification of human B cells (CD19), T cells (CD3), monocytes (CD33+CD11c+), dendritic cells (CD33−CD11c+), and NK cells (CD33−CD56+) in the blood, spleen, and bone marrow of humanized Rag2/γc/FcRγ−/− mice within the hCD45+ cell population.

(B) Identification of different B cell developmental stages in the bone marrow, spleen, and blood of humanized Rag2/γc/FcRγ−/−mice.

(C) Percentage of pro-, pre-, immature, and mature B cell subpopulations in the bone marrow of humanized Rag2/γc/FcRγ−/− mice within the human B cell population (hCD45+CD19+).

(D) Quantification of serum IgM and IgG levels in humanized Rag2/γc/FcRγ−/− mice 16 weeks posttransplantation.

(E) Presence of cell-surface-associated IgG on human B cells (CD19+) and human monocytes (CD33+) in the blood of humanized Rag2/γc/FcRγ−/− mice as detected by flow cytometry.

(F) Presence of the human complement component C3 in human serum and in the serum of humanized Rag2/γc/FcRγ−/− and C57BL/6 mice.

All experiments were done with animals at 12–16 weeks posttransplantation with human HSCs and at least nine animals per group. Bar graphs indicate the mean value ± SD. Horizontal lines indicate the statistical mean.

See also Figure S1 and Table S1.

completely eradicate all mouse hematopoietic cells. Therefore, to generate an immunodeficient mouse strain that does not express mouse activating FcγRs, we crossed the Rag2/γc−/− mouse strain, which is known to efficiently accept human hematopoietic cells, with the FcRγ-deficient mouse, thereby creating Rag2/γc/FcRγ−/− mice. As shown in Figures 1C and 1D, these animals lack mouse B and T cells, and do not express mouse activating FcγRs on innate immune effector cells, such as neutrophils and monocytes, resulting in abrogated activity of the 6A6-hIgG1 antibody (Figure 1B). Thus, upon reconstitution of Rag2/γc/FcRγ−/− mice with a human immune system, only human innate immune effector cells will express human activating FcγRs, which allowed us to exclude the contribution of residual mouse innate immune effector cells beyond any doubt.

Reconstitution of a Human Immune System in Rag2/γc/FcRγ−/− Mice

Next, we established the experimental conditions for reconstitution of Rag2/γc/FcRγ−/−mice with human HSCs. Irradiation of newborn mice with 6 Gy resulted in the highest level of reconstitution with human hematopoietic cells in the peripheral blood of individual mice 12 weeks after transplantation (Figure S1A). As previously described for other immunodeficient mouse strains, in addition to the blood, human cells were abundantly present in the spleen and bone marrow of the reconstituted animals (Figure S1B; Table S1; Shultz et al., 2012; Tanaka et al., 2012; Traggiai et al., 2004). Moreover, the level of reconstitution did not impact the cell lineages present in these animals, as B cells, T cells, monocytes, and NK cells could be found at comparable levels in mice with a low or high reconstitution level (Figures S1C and S1D). A more detailed analysis of human cell types present in the blood, spleen, and bone marrow of transplanted animals identified T cells, monocytes, NK cells, and dendritic cells, as well as B cells in early and late differentiation stages, including pro- (CD34+CD19+CD10+IgM−), pre- (CD34−CD19+CD10+IgM−), immature (IgM+CD19+CD10+), and mature (IgM+CD19+CD10−) B cells (Figures 2A–2C), in line with previous reports (Blom and Spits, 2006; Ghia et al., 1998; Tanaka et al., 2012; Traggiai et al., 2004). Consistent with the presence of B cells, serum IgM and IgG were present in the serum of mice, albeit at much lower levels than in human serum (Figure 2D). However, this amount seemed sufficient to result in binding to CD33+ myeloid cells, most likely via the

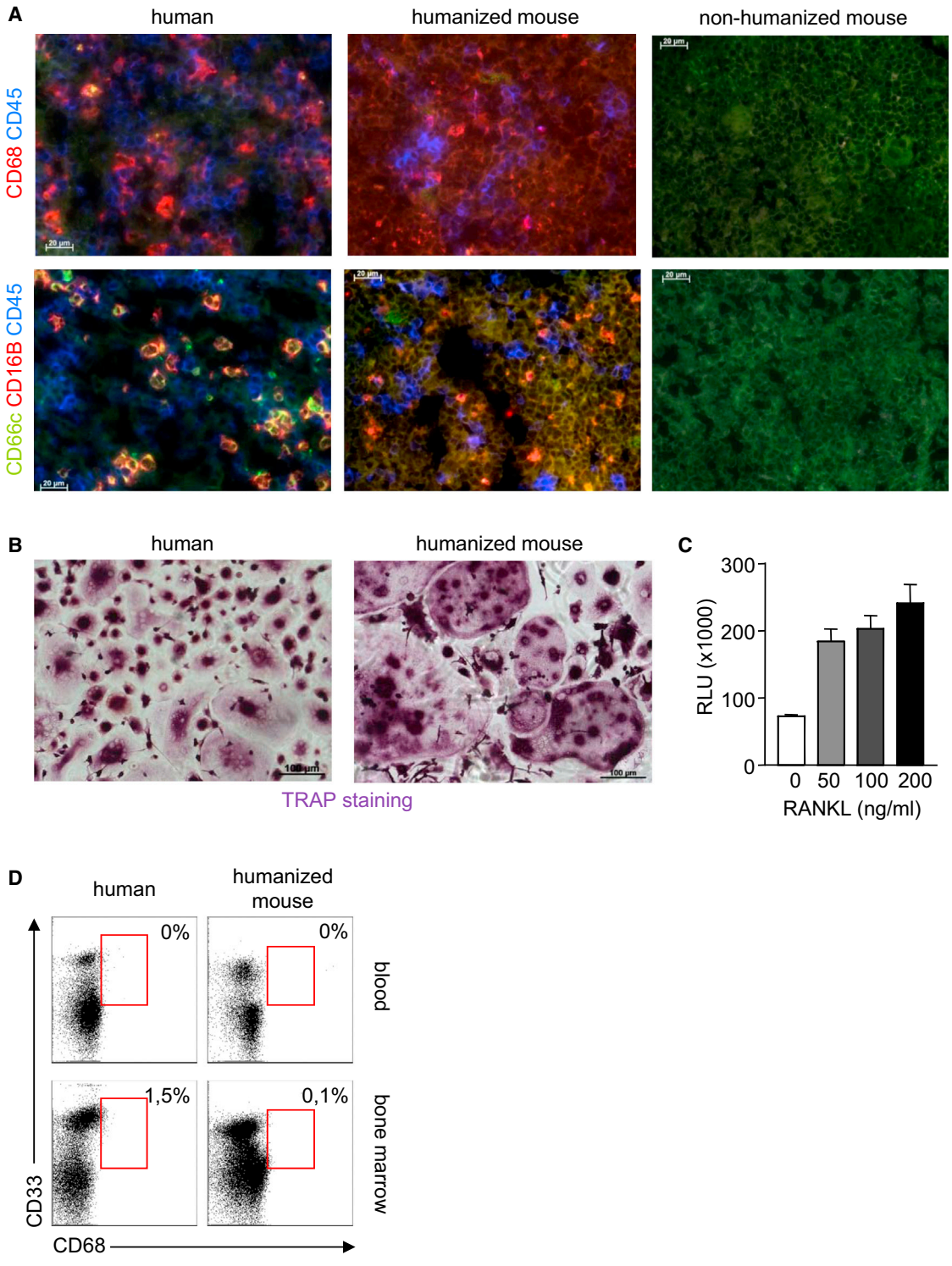

Figure 3. Presence of Human Macrophage and Neutrophil Populations in Humanized Mice

(A) Immunofluorescence analysis of spleen sections of humans, humanized mice, and nonhumanized mice stained with CD68 to identify macrophages and CD66c in combination with CD16B to identify neutrophils. CD45 was used to identify human hematopoietic cells.

(B) Cultures of human PBMCs or bone marrow cells of humanized mice in the presence of M-CSF and RANKL to initiate osteoclast development. The purple staining identifies the osteoclast-associated enzyme TRAP.

(legend continued on next page)

high-affinity FcγRI expressed on this cell type (Figures 2E and 4A). In contrast to the presence of all essential cell types important for IgG-dependent effector functions, these mice did not produce significant levels of human complement, consistent with the important role of nonhematopoietic tissues, such as the liver, for the generation of complement proteins (Figure 2F). Furthermore, CD66c/CD16B+ neutrophils and CD68+ macrophages were abundantly present in the spleen of humanized mice, as demonstrated previously in other humanized immunodeficient mouse strains (Figure 3A; Tanaka et al., 2012). Since others have demonstrated that these human macrophages are functional with respect to cytokine secretion and phagocytic function (Tanaka et al., 2012), we turned our attention to another bone resident macrophage population, namely, osteoclasts, which had not previously been investigated in humanized mice. First, we cultured bone marrow of humanized mice and human PBMCs with macrophage colony-stimulating factor (M-CSF) and receptor activator of NF-κB ligand (RANKL), which drives monocyte precursors into the osteoclast lineage (Nakashima et al., 2012). As shown in Figure 3B, this indeed resulted in the generation of mature osteoclasts, identified by large multinucleated cells expressing the osteoclast marker tartrate-resistant acid phosphatase (TRAP). More importantly, these osteoclasts were fully functional, as demonstrated by their capacity to resorb bone matrix (Figure 3C). In contrast to the presence of human macrophages in the spleen, no CD68-expressing cells were detectable in the bone marrow and blood of the humanized mice and humans (Figure 3D).

A prerequisite for studying human IgG-dependent effector functions in humanized mice is the presence of human FcγRs on innate immune effector cells. In humans, FcγRIIIA is the only activating FcγR expressed on NK cells, whereas monocytes and macrophages express a broader repertoire of activating FcγRs (Hogarth, 2002; Ravetch and Nimmerjahn, 2008). As shown in Figure 4A, NK cells expressing FcγRIIIA and monocytes positive for FcγRIA, FcγRIIA, FcγRIIB, and FcγRIIIA were present in the blood, spleen, and bone marrow of these animals. In combination with FcγRIIIB expression on human neutrophils (Figure 3A), this suggests that all relevant human FcγRs are expressed on innate immune effector cells. This cell-type-specific pattern of FcγR expression was consistent with the presence of these receptors on CD33+ monocytes in the respective human organs (Figure 4B), suggesting that human FcγR expression is fully recapitulated in the humanized Rag2/γc/FcRγ$-/-$ mice. In a notable exception, there was a low level of FcγRIIB expression on monocytes in the peripheral blood of humanized mice, whereas their counterparts in the human blood were mostly negative for this receptor.

Activity of Human CD20-Specific IgG Subclasses in Humanized Mice

Because CD20 is the major target for therapeutic B cell-depleting antibodies, we next assessed the CD20 expression pattern on human B cells developing in humanized mice and humans (Johnson and Press, 2000; Sanz and Lee, 2010). As shown in Figure 5A, CD20 was highly expressed on all IgM+ B cell populations in the blood, spleen, and bone marrow of humanized mice. In contrast, pro- and pre-B cell populations expressed only very small amounts of CD20, whereas the majority of immature B cells were strongly positive for this marker. Of note, mouse CD20 has been demonstrated to be absent from pro-B and the vast majority of pre-B cells, and to be expressed only starting from the very late pre-B to immature B cell stage. Interestingly, this mouse-specific expression pattern was recapitulated in transgenic mice expressing human CD20, further emphasizing the need for humanized mouse models to fully match the human expression pattern especially during early B cell development (Gong et al., 2005; Uchida et al., 2004b).

As a CD20-specific therapeutic antibody, we chose the hybridoma clone 1F5, which was used in early human clinical trials to deplete B cells in its mouse IgG2a form, and generated all four human IgG subclass switch variants of this antibody (Johnson and Press, 2000). Upon injection of equal amounts of these IgG switch variants into humanized mice (10 μg per mouse), we could show that the 1F5-IgG1, 1F5-IgG2, and 1F5-IgG3 variants were more efficient in reducing B cell counts compared with 1F5-IgG4 (Figures 5B–5D). Importantly, this different level of activity could not be explained by a different half-life of these IgG switch variants in humanized mice in vivo (Figure S2A). In a similar manner, the amount of human cells present in these animals did not correlate with the level of B cell depletion (Figures S2B–S2D). Of note, although human IgG4 is widely considered not to have any cytotoxic activity, it clearly had the capacity to deplete B cells, which is consistent with recent in vitro studies demonstrating that especially large IgG4 immune complexes can indeed bind to FcγRs, such as FcγRI (Bruhns et al., 2009; Lux and Nimmerjahn, 2011). Overall, the observed differences in in vivo activity are in line with previous results obtained in classical mouse models, which demonstrated that the activity of IgG subclasses in vivo correlates with their affinity for different FcγRs (Fossati-Jimack et al., 2000; Hamaguchi et al., 2006; Nimmerjahn and Ravetch, 2005). With respect to the kinetics of B cell depletion, the majority of B cells were absent from the peripheral blood of humanized mice 24 hr after anti-CD20 injection (Figure 5C). Especially for the IgG1 and IgG2 switch variants, B cell depletion was long lasting and B cell counts did not return to normal levels over the observation period of the experiment (Figure 5D). Similar results have been obtained in murine models of B cell depletion with CD20-specific antibodies and in human patient cohorts treated with rituximab (Figure S2E; Hamaguchi et al., 2006; Sanz et al., 2007; Uchida et al., 2004a; Beers et al., 2008). Of note, B cell depletion was fully dependent on the IgG Fc fragment, as neither $F(ab')_2$ fragments nor deglycosylated variants of the same antibody were able to induce a reduction in B cell counts (Figures 5E and 5F). These findings support the notion that despite the capacity of antibodies against CD20

(C) Assessment of the capacity of osteoclasts generated from the bone marrow of humanized mice in the presence of M-CSF and the indicated concentrations of RANKL to resorb bone matrix.

(D) Analysis of humanized mouse or human blood and bone marrow to detect CD68+ macrophages. All experiments were done with animals at 12–16 weeks posttransplantation with human HSCs and at least two animals per group. Bar graphs indicate mean value ± SD.

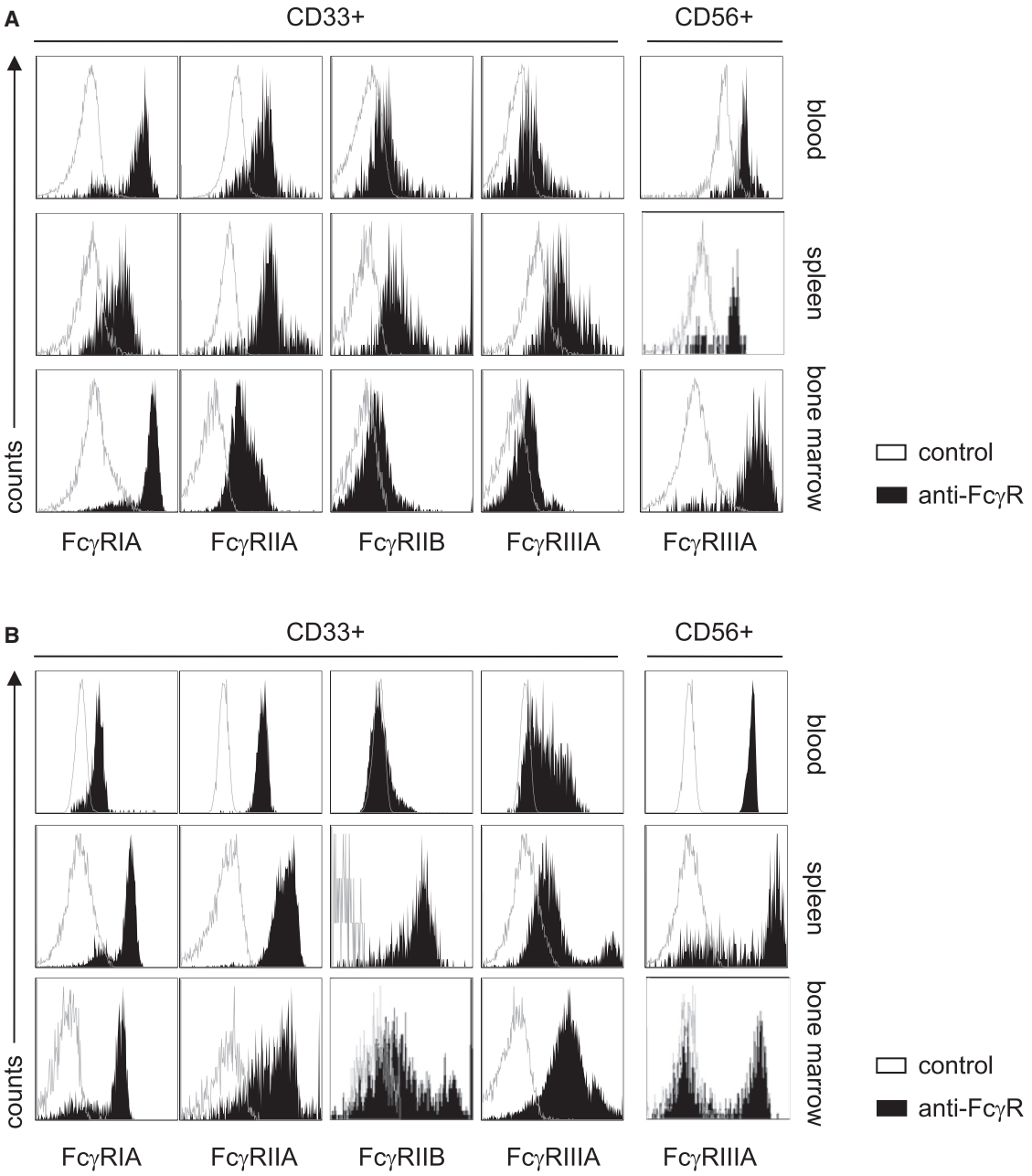

Figure 4. Expression of Human FcγRs on Innate Immune Effector Cells

Expression of the indicated human FcγRs on CD33+ monocytes and CD56+ NK cells in the blood, spleen, and bone marrow of humanized Rag2/γc/FcRγ−/− mice (A) or humans (B) as determined by flow cytometry. Depicted is a representative result from nine independent animals at 12–16 weeks posttransplantation or a minimum of three independent human samples. Cells from five humanized mice were pooled for staining of FcγR expression on peripheral blood cells.

to directly inhibit B cell proliferation and induce apoptosis without secondary crosslinking in vitro, the IgG Fc fragment is crucial for anti-CD20-dependent B cell depletion in vivo (Bonavida, 2007; Shan et al., 1998).

To determine whether FcγR allelic variants represented in the HSCs used to reconstitute the mice with a human immune system might explain some of the differences in antibody activity observed between the higher- and lower-responder mice, we genotyped the donors (Table S2) and color-coded all of the mice that carried specific FcγRIIA high/low affinity and FcγRIIIA high/low affinity alleles. As shown in Figures 5C and 5D, this did not show a clear correlation with the activity of antibody-mediated B cell depletion. Similar results were obtained in human lymphoma patients before and after treatment with rituximab, suggesting that B cell depletion is not affected by differences in FcγR allelic variants, at least at the studied antibody

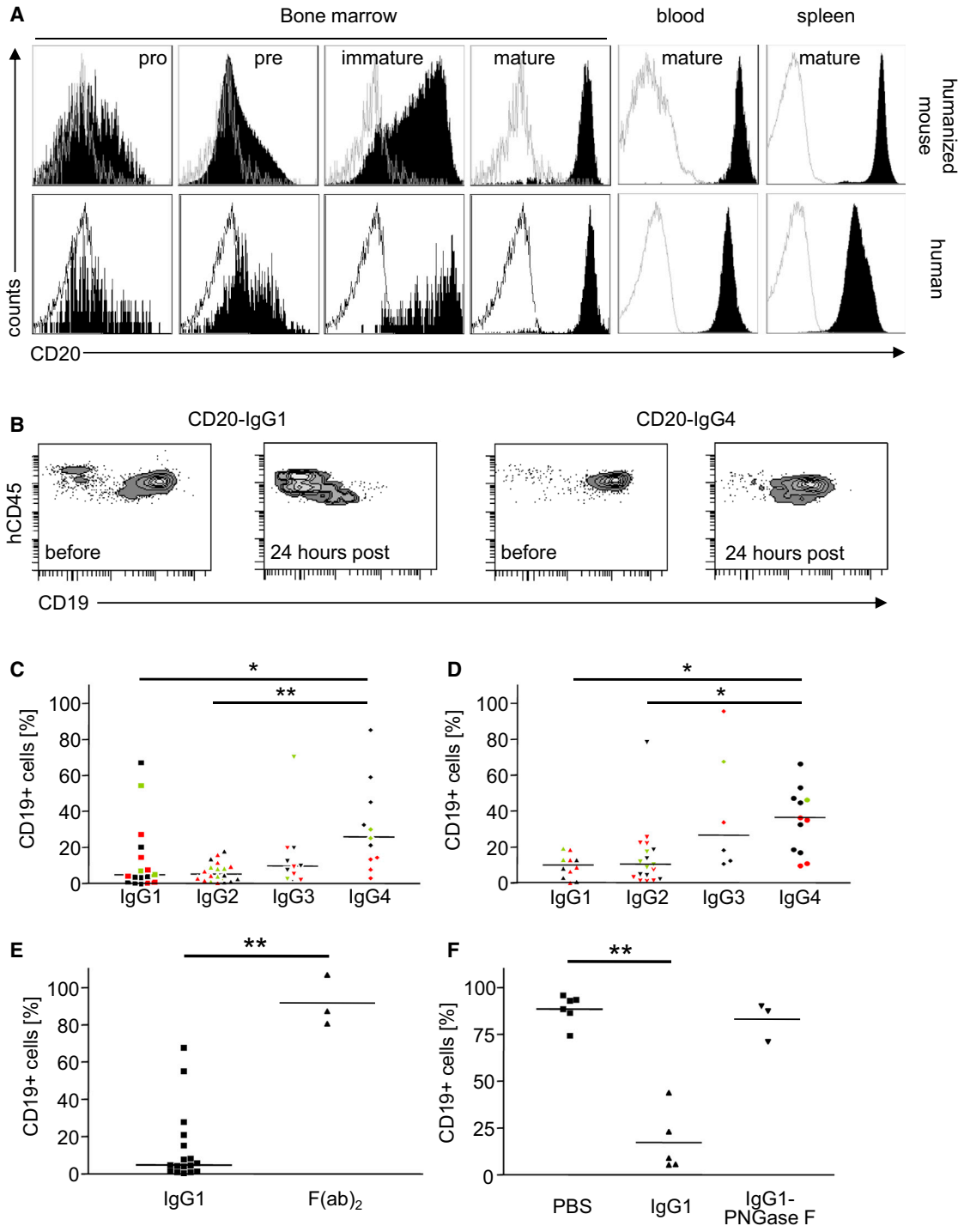

Figure 5. Anti-CD20 IgG-Mediated B Cell Depletion in Humanized Mice

(A) Detection of CD20 expression on pro- (CD45+CD19+CD10+CD34+IgM−), pre- (CD45+CD19+CD10+CD34−IgM−), immature (CD45+CD19+CD10+CD34−IgM+), and mature B cells (CD45+CD19+CD10−CD34−IgM+) in the bone marrow (BM) and on mature B cells in the blood and spleen of humanized mice and humans via flow cytometry.

(B) Representative example of the differential capacity of the CD20-specific 1F5-IgG1 and 1F5-IgG4 switch variants to deplete B cells (CD19+) in peripheral blood of humanized mice 24 hr after antibody administration.

(C and D) Groups of humanized mice (n = 11–20) were injected with 10 μg of the indicated 1F5 IgG variant, and B cell depletion in the peripheral blood was assessed at 1 (C) or 7 (D) days after anti-CD20 injection. The FcγRIIA-131H/R and FcγRIIIA-158F/V genotype of the donors was determined. Low-affinity donors

(legend continued on next page)

concentration in the blood of humanized mice and humans (Figure S2E). In addition to the blood, we also investigated the capacity of the IgG1 switch variant to deplete B cells in the spleen and bone marrow. As shown in Figures 6A–6C, a single injection of 1, 10, and 100 μg anti-CD20 IgG1 efficiently depleted mature B cells in the blood and spleen. In contrast, depletion of mature B cells in the bone marrow was less efficient and required an at least 10-fold higher antibody dose (Figure 6D). Even more striking, although the immature B cells expressed CD20 to a level comparable to that observed in mature B cells, they never reached a significant level of depletion. The same applied for pro- and pre-B cells, although these B cell subsets clearly expressed much lower amounts of this cell-surface marker (Figures 5A and 6D). Again, no clear correlation with the allelic variants of activating FcγRs was notable (Table S3). A possible explanation for this phenomenon might be a lower availability of the therapeutic CD20-specific antibody in the bone marrow. To address this question experimentally, we injected a fluorescently labeled aglycosylated version of the CD20-specific antibody to prevent the rapid depletion of anti-CD20-coated B cells in the blood and spleen. As shown in Figures 6E and 6F, all mature B cell populations were labeled by the injected antibody regardless of their anatomical localization. In line with the comparable level of CD20 expression, immature B cells displayed the same amount of therapeutic antibody binding as mature B cells. As expected, pro- and pre-B cells were stained at a lower but still clearly detectable level. Another reason for this reduced level of B cell depletion may be the lack of responsible innate immune effector cells. As shown in Figures 2A and 4A, however, NK cells and CD33+ myeloid cells were present in the bone marrow. A more detailed analysis of the CD33+ cells in the bone marrow revealed that the majority of these were negative for c-kit and CD34, and thus represent more mature CD14 high- and low-monocyte subsets, as expected (Figure 6G). In contrast to monocytes, CD68+ macrophages were present only in very low amounts in the bone marrow or virtually absent in the blood from humanized mice and humans (Figure 3D). To further validate this observation, we analyzed the efficacy of B cell depletion in the bone marrow of C57BL/6 mice with an antibody specific for mouse CD20. Again, the depletion of immature B cells required a much higher dose, despite a similar binding of the CD20-specific antibody compared with mature B cells, which were depleted with a similar efficacy compared with the blood and spleen (Figure S3), in line with previous reports. In contrast to what was observed in humans and humanized mice, pro-B and pre-B cells in C57BL/6 mice did not express CD20, and accordingly could not be recognized via the CD20-specific antibody (Figure S3B). Therefore, it was not possible to assess their depletion, providing yet another argument for the necessity of a humanized mouse model.

DISCUSSION

Taken together, our results provide evidence that Rag2/γc/FcRγ−/− mice might be a valuable tool for studying human IgG activity in a preclinical setting in vivo. Compared with injecting human PBMCs into immunodeficient Rag2/γc−/−, NOD/SCID, or NOD/SCID/γc−/− mice, which are frequently used as surrogate humanized mouse models to study human IgG activity, this mouse model has several advantages (Goldman et al., 1998; Ito et al., 2002). Most importantly, mouse innate immune effector cells in Rag2/γc/FcRγ−/− mice no longer have functional activating FcγRs, which allowed us to study the interaction of human antibodies with human target and effector cells in vivo. Our work reveals that human IgG4 antibodies are able to deplete target cells, and is fully consistent with recent in vitro studies (Bruhns et al., 2009; Lux et al., 2013). Moreover, the presence of B cells in all developmental stages expressing physiological levels of the target antigen in all relevant organ structures and niches is not reflected in the NOD/SCID model system reconstituted with human PBMCs in the peritoneum. Similar arguments apply to transgenic mouse models that express human B cell antigens, such as human CD19 and CD20, on mouse B cells (but lack human innate immune effector cells), and to mice that are transgenic for all human FcγRs, in which human serum antibodies and the target human antigen are not present (Beers et al., 2008; Gong et al., 2005; Yazawa et al., 2005; Smith et al., 2012). Of note, the expression pattern of human CD20 on early mouse B cell progenitors in the bone marrow of human CD20 transgenic mice seems to mimic the expression pattern of mouse CD20, being virtually absent from pro-B and pre-B cell stages (Gong et al., 2005; Uchida et al., 2004b). In contrast, the expression of human CD20 in humanized Rag2/γc/FcRγ−/− mice fully resembled the human expression pattern. Another attractive feature is the long-term reconstitution with human immune cells, which may allow the activity of therapeutic antibodies to be monitored over a longer observation period compared with the transient availability of human cell subsets in PBMC-reconstituted animals. Despite these advantages, however, there are also obvious disadvantages, including the variability in reconstitution and the genetic heterogeneity among donors. This may require larger groups of animals to obtain conclusive results, but in the end might mimic the human situation more closely. The other point to be considered is that the human immune system in humanized mice represents a 4- to 6-month-old developmental stage and thus may not fully be comparable to the immune system of an adult human. This may explain at least in part some of the differences we observed with respect to the level of FcγR expression and the overrepresentation of certain cell types, primarily B cells, especially early after reconstitution.

(HR-FF, RR-FF, and RR-FV) are depicted in red, medium-affinity donors (HR-FV) are shown in black, and high-affinity donors (HR-VV, HH-FV, and HH-VV) are shown in green.

(E) Groups of humanized mice were injected with intact anti-CD20 IgG1 or an anti-CD20 $F(ab)_2$ fragment, and B cell counts were assessed 1 day after antibody injection.

(F) Peripheral blood B cell counts in humanized mice 24 hr after injection of PBS, intact 1F5, or aglycosylated 1F5 antibody (PNGaseF). Statistical analysis was performed by Kruskal-Wallis test and subsequent post hoc tests. Asterisks indicate values with a significant difference. *$p < 0.05$, **$p < 0.01$.

See also Figure S2 and Table S2.

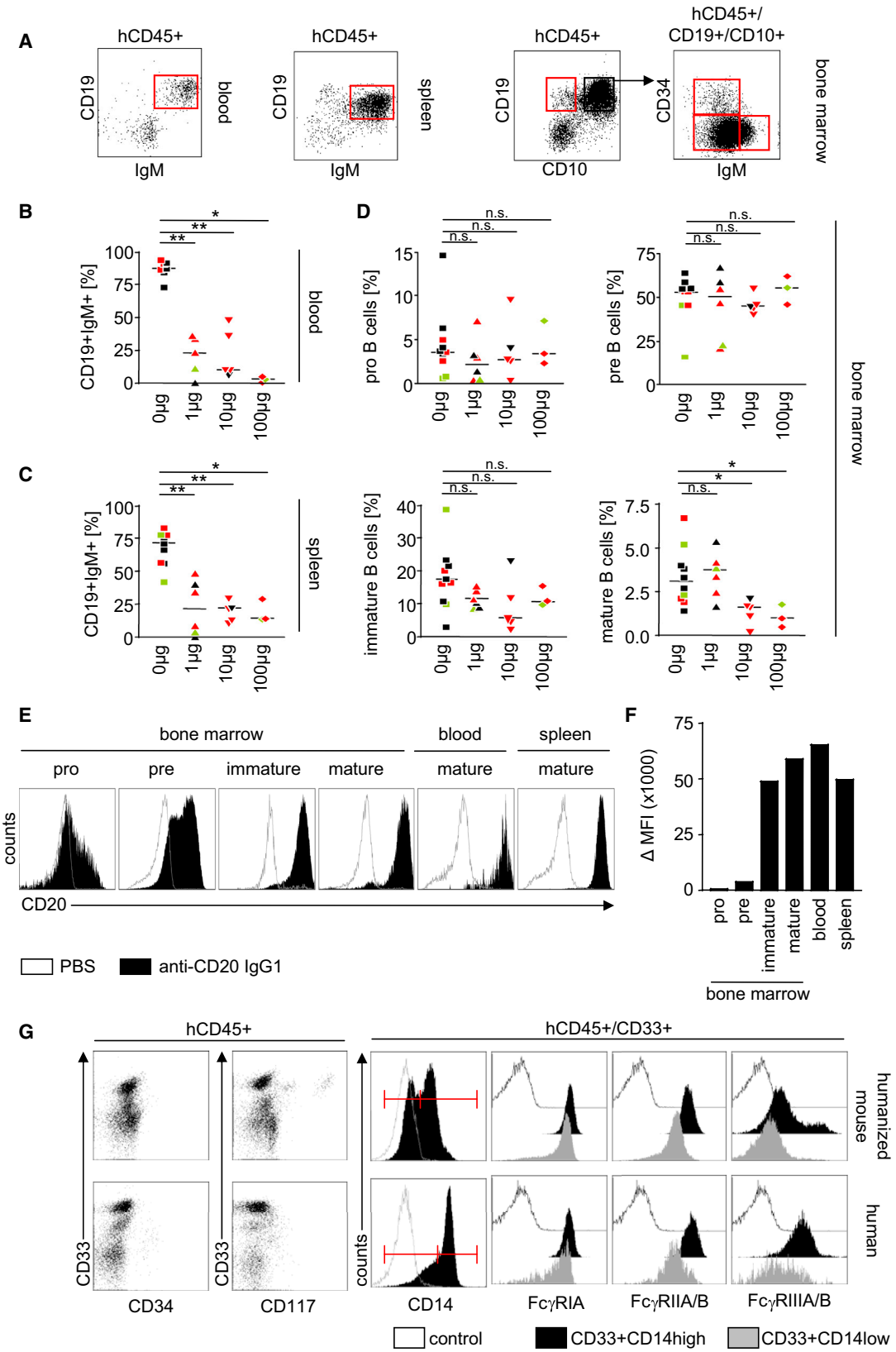

(legend on next page)

By studying antibody-dependent B cell depletion in this model system, we were able to show that the efficacy of target cell depletion varied greatly depending on the anatomical site. Thus, whereas mature B cells of the peripheral blood and the spleen were depleted very effectively even by small antibody doses, an at least 10-fold higher amount of antibody was required to deplete mature B cells in the bone marrow. Although immature B cells expressed only slightly lower levels of CD20 compared with mature B cells and were bound by the same amount of cytotoxic antibody, they did not become depleted efficiently even at high antibody doses, suggesting that the bone marrow may represent a niche with low antibody-dependent cell-mediated cytotoxicity (ADCC) activity. An alternative but nonmutually exclusive explanation is that immature B cells are somehow resistant to antibody-mediated depletion. A similar but less pronounced effect could be observed in a model system of anti-CD20-mediated depletion of mouse B cells, in which a 5-fold higher dose was required to deplete immature B cells effectively, consistent with earlier results (Hamaguchi et al., 2005). Further along these lines, immature mouse B cells expressing human CD20 as a transgene showed a similar resistance to anti-CD20-dependent depletion (Gong et al., 2005). The higher ADCC activity toward mature mouse B cells may be explained at least in part by the much higher affinity of the mouse IgG2a antibody subclass for the respective murine activating FcγRI and FcγRIV, which are responsible for B cell depletion in the mouse (Biburger et al., 2011; Hamaguchi et al., 2006; Beers et al., 2010). With respect to earlier B cell subsets, which were also bound by the CD20 antibody, their much lower expression of CD20 may explain at least in part their resistance to depletion. As this was not the case for immature B cells, however, other explanations have to be considered. Apart from antibody availability, a lack of effector cells required for B cell killing may have the same effect on ADCC efficacy. CD16+ NK cells, however, were abundantly present in the bone marrow. Moreover, CD33/CD16+ monocytes negative for the early monocyte precursor markers CD34 and CD117 were present in the bone marrow and have the capacity to develop into fully functional human macrophages (Tanaka et al., 2012; Li et al., 2013). It remains possible, however, that although monocytes express all relevant activating FcγRs and are involved in ADCC reactions in the blood, they may not be involved in ADCC reactions in the bone marrow. Alternatively, macrophages have been implicated as ADCC effector cells in other tissues, such as the liver (Montalvao et al., 2013; van der Bij et al., 2010). In the bone marrow of humanized mice and humans, only very few CD68+ cells could be detected, which may provide an alternative explanation for the lower ADCC activity. Since a small level of cell depletion could be achieved at high antibody doses, it will be interesting to investigate the capacity of ADCC-enhanced antibodies (e.g., lacking branching fucose residues) to efficiently deplete B cells in the bone marrow.

Thus far, we have not observed a correlation between the efficacy of B cell depletion in the peripheral blood and spleen of humanized mice or humans and the presence of high- or low-affinity FcγRIIA and IIIA alleles, which have been correlated with a better therapeutic outcome for lymphoma or breast cancer patients undergoing antibody therapy (Cartron et al., 2002; Musolino et al., 2008; Weng et al., 2004; Weng and Levy, 2003). To obtain more informative results, we may need to focus on larger humanized mouse colonies that exclusively carry either the high- or low-affinity allelic variants of FcγRIIIA and FcγRIIA, respectively, and study B cell depletion especially in the bone marrow. Altogether, this humanized mouse model should allow a more detailed understanding of human IgG activity on the background of a human immune system, and may become a valuable preclinical test system to validate IgG-based immunologicals. Given the capacity of human myeloid precursor cells to develop into human osteoclasts, this mouse model may also be suitable for investigating autoantibody-mediated bone loss in human serum transfer arthritis models.

EXPERIMENTAL PROCEDURES

Mice

C57BL/6 mice were bought from Janvier, and Balb/c-Rag2/γc−/− (Rag2/γc−/−) mice were provided by Hergen Spits (AMC Amsterdam). FcγRI-deficient mice (FcγRI−/−) and FcγRIV-deficient mice (FcγRIV−/−) on the C57BL/6 background, as well as *fcer1g*-deficient mice (FcRγ−/−) on the Balb/c and C57BL/6 backgrounds, were provided by Jeffrey Ravetch (Rockefeller University) and Mark Hogarth (Burnet Institute). Balb/c-Rag2/γc/FcRγ−/− (Rag2/γc/FcRγ−/−) mice were generated by crossing Balb/c-Rag2/γc−/− with Balb/c-FcRγ−/− animals followed by breeding to a homozygous deletion for all three respective genes. Mice were kept in the animal facilities of Friedrich-Alexander-University Erlangen-Nürnberg and Rockefeller

Figure 6. Efficiency of Anti-CD20-Dependent Depletion in Different Tissues

(A) Flow-cytometry analysis to identify B cell populations in blood (CD45+CD19+IgM+), spleen (CD45+CD19+IgM+), and bone marrow (pro B cells: CD45+CD19+CD10+CD34+IgM−; pre B cells: CD45+CD19+CD10+CD34−IgM−; immature B cells: CD45+CD19+CD10+CD34−IgM+; mature B cells: CD45+CD19+CD10−CD34−IgM+) of humanized Rag2/γc/FcRγ−/− mice.

(B–D) Quantification of the indicated B cell subpopulations within human CD45+ cells in humanized Rag2/γc/FcRγ−/− animals treated with the different amounts of anti-CD20 IgG1 or PBS in blood (B), spleen (C), and bone marrow (D) by flow cytometry 1 day after antibody injection. The FcγRIIA-131H/R and FcγRIIIA-158F/V genotype of the HSCs used to reconstitute the mice was determined. Low-affinity donors (HR-FF, RR-FF, and RR-FV) are depicted in red, medium-affinity donors (HR-FV) are shown in black, and high-affinity donors (HR-VV and HH-VV) are shown in green. Horizontal lines indicate the statistical median. Statistical analysis was performed by ANOVA. If statistical differences were detected, subsequent Mann-Whitney tests were performed to compare untreated (0 μg) and treated (1 μg, 10 μg, 100 μg) groups. Multiple comparisons were corrected for by the Bonferroni method. Asterisks indicate values with significant difference. *$p < 0.05$, **$p < 0.01$ (according to Bonferroni correction of three comparisons). n.s., not significant.

(E and F) Binding (E) and quantification of the binding (F) of 10 μg A647-labeled aglycosylated anti-CD20 IgG1 to the indicated B cell populations in vivo in blood, spleen, and bone marrow 1 day after application as compared with injection of PBS.

(G) Flow-cytometry analysis of humanized mouse (n = 3) or human (n = 3) bone marrow CD33+ cell populations within the hCD45+ population. Human FcγR expression was compared between $CD14^{high}$- and $CD14^{low}$-expressing CD33+ cells. Shown is one out of three representative independent experiments.

See also Figure S3 and Table S3.

University under specific pathogen-free conditions in individually ventilated cages according to the guidelines of the National Institutes of Health and the legal requirements of Germany and the United States. Immunodeficient Rag2/γc−/− and Rag2/γc/FcRγ−/− mice were supplied with acidified drinking water (pH 3.0) to minimize the risk of bacterial infections in these heavily immunocompromised mouse strains.

Generation of Humanized Mice

Newborn Rag2/γc/FcRγ−/− mice were irradiated at the indicated doses and injected intravenously with 50,000–80,000 human HSCs 4–6 hr after irradiation. HSCs were purified from umbilical cord blood with the written consent of patients and according to the ethical guidelines of the University of Erlangen-Nürnberg and the Klinikum Fürth. In brief, PBMCs were isolated by density centrifugation and CD34+ HSCs were purified using the Direct CD34 Progenitor Cell Isolation Kit, human (Miltenyi Biotec) according to the manufacturer's instructions. Isolated HSCs were frozen and stored in liquid nitrogen until further use.

In Vivo Platelet Depletion Assay

The ability of murine activating FcγR to mediate human IgG effector functions was analyzed by intravenous injection of 10 μg of a humanized anti-platelet (clone 6A6-hIgG1) in C57BL/6, FcRγ−/−, FcγRI−/−, and FcγRIV−/− mice (all on the C57BL/6 background), and in Rag2/γc−/− and Rag2/γc/FcRγ−/− mice. As described previously, platelet counts in the peripheral blood of individual mice were assessed before and 4 hr after 6A6-hIgG1 injection with the use of an Advia120 Hematology System (Siemens) (Nimmerjahn and Ravetch, 2005).

Fluorescence-Activated Cell Sorting Analysis

Fluorescence-activated cell sorting (FACS) analysis was conducted with PBMCs isolated from the peripheral blood of humanized mice and human cancer patients, with their written consent and according to the ethical guidelines of the University of Erlangen-Nürnberg, by Ficoll density gradient centrifugation. For bone marrow and spleen, we prepared single-cell suspensions before proceeding to FACS analysis. The following antibodies were used for staining of murine PBMCs and FcγRs in C57BL/6, Rag2/γc−/−, and Rag2/γc/Fcγ−/− mice: APC-conjugated B220 (clone RA3-6B6) PerCP-conjugated B220 (clone RA3-6B6), fluorescein isothiocyanate (FITC)-conjugated TCRβ (clone H57-597), PerCP-Cy5.5-conjugated CD11b (clone M1/70), PE-conjugated CD16/CD32 (clone 2.4G2), biotin-conjugated CD45.2 (clone 104), CD64 (clone X54-517.1), PE-Cy7-conjugated CD62L (clone MEL-14), FITC-conjugated IgD (clone 11-26c.2a), APC-conjugated GR-1 (clone RB6-8C5), FITC-conjugated Ly6G (clone 1A8), biotinylated IgM (clone II/41), and PE-conjugated CD43 (clone Ly-48) (all purchased from BD Pharmingen). APC-H7-conjugated CD45 (clone 30-F11) was purchased from BioLegend. PE-conjugated CD16 (clone 275003) was purchased from R&D. PE-conjugated Nkp46 (clone 29A1.4) and PE-7-conjugated CD19 (clone 1D3) were purchased from eBioscience. The following antibodies (purchased from BD Pharmingen) were used for staining of human cells and FcR in humanized Rag2/γc/Fcγ−/− mice: PerCP-conjugated CD3 (clone UCHT1), FITC-conjugated CD10 (clone HI10a), PerCP-conjugated CD14 (clone M5E2), FITC-conjugated CD16 (clone 3G8), PE-conjugated CD16 (clone 3G8), PE-conjugated CD16B (clone CLB-gran11.5), PE-conjugated CD19 (clone HIB19), PE-Cy7-conjugated CD19 (clone SJ25C1), PE-Cy7-conjugated CD33 (clone P67-6), PE-conjugated CD34 (clone 8.G12), PerCP-conjugated CD45 (clone 2D1), APC-conjugated CD45 (clone HI30), APC-H7-conjugated CD45 (clone 2D1), PE-conjugated CD56 (clone NCAM16.2), FITC-conjugated CD64 (clone 10.1), purified CD66c (clone B6.2/CD66), PE-conjugated CD68 (clone Y1/82A) PE-conjugated CD117 (clone 104D2), biotinylated IgD (clone IA6-2), biotinylated IgM (clone G20-127), and PE-conjugated IgM (clone G20-127). FITC-conjugated CD11c (clone 3.9) was purchased from eBioscience. Alexa647-conjugated CD32 (clone FUN-2) and PerCP-conjugated CD56 (clone HCD56) were purchased from BioLegend. PE-conjugated human IgG was purchased from Jackson ImmunoResearch. APC-Cy7-conjugated streptavidin for detection of biotinylated primary antibodies was purchased from BD Pharmingen. The following antibodies were produced in our laboratory: murine Alexa647-conjugated FcγRIV (clone 9E9), human biotinylated CD32B (clone 2B6), human FITC-conjugated CD20 (clone 1F5), and human A647-conjugated CD20 (clone 1F5). FACS staining was generally conducted in the presence of unlabeled CD16/CD32 antibody (clone 2.4G2; Serotec) as a murine Fc blocking reagent, except for direct analysis of murine FcγRs. To increase the cell number of rare cell populations, such as NK cells, in the peripheral blood of humanized mice, blood from several animals was pooled. Experiments were acquired on a FACSCantoII (BD) and analyzed using FACSDiva or FlowJo software.

Cloning and Production of Antibodies

Human anti-CD20 IgG (clone 1F5) switch variants were generated as previously described (Nimmerjahn and Ravetch, 2005). In brief, total RNA was isolated from the 1F5 hybridoma cell line (obtained from ATCC) and subjected to 5′-RACE using the 5′RACE System for Rapid Amplification of cDNA ends (Invitrogen) according to the manufacturer's instructions. The sequences of the specific primers were as follows: 5′-gac agg gat cca gag tt-3′ (IgG2a heavy-chain gene-specific primer 1), 5′-gta ctc tag agg tca agg tca ctg gct ca-3′ (IgG2a heavy-chain gene-specific primer 2), 5′-cct gtt gaa gct ctt gac a-3′ (k light-chain gene-specific primer 1), and 5′-gta ctc tag agg gtg aag ttg atg tct tgt c-3′ (k light-chain gene-specific primer 2). The light- and heavy-chain variable regions were cloned in pCR-Topo-Blunt (Invitrogen) and confirmed by sequencing. Primers for PCR amplification of variable regions and subsequent cloning were derived from the resulting sequence information: 5′-cgt aga att cac cac cat ggg atg gag ttg tat cat c-3′ (1F5 VH) and 5′-cgt aga att cac cac cat gga ttt tca agt gca gat tt-3′ (1F5 VL). The heavy-chain variable region was fused to heavy-chain constant regions of the human IgG subclasses and cloned into the eukaryotic pBos expression vector via EcoRI and KpnI restriction sites. The kappa light-chain variable region was fused to the human kappa light-chain constant region and cloned in the pCMV vector via NcoI and XhoI restriction sites. Antibodies were produced by transient transfection in HEK293T cells and subsequent isolation from the cell culture supernatant by ammonium sulfate precipitation and protein G purification as previously described (Nimmerjahn and Ravetch, 2005). The integrity of the produced switch variants was confirmed by reducing PAGE. The $F(ab)_2$ fragment of the antibody was generated by digestion with pepsin for 2 hr at 37°C in a buffer of 0.1 M sodium citrate (pH 3.5) followed by dialysis against PBS. Deglycosylation of anti-CD20 IgG was achieved by digestion with 50 U/μg PNGase F overnight at 37°C.

Anti-CD20 IgG-Induced B Cell Depletion In Vivo

Anti-CD20 IgG switch variants were intravenously injected into 12- to 16-week-old humanized Rag2/γc/FcRγ−/− mice at the indicated amounts. B cell counts in peripheral blood were analyzed by flow cytometry before and 1 and 7 days after antibody injection. B cell counts in spleen and bone marrow were analyzed 1 day after antibody application.

ELISA-Based Assays

Serum of humanized Rag2/γc/FcRγ−/− mice was analyzed for the presence of human C3 protein by a sandwich ELISA using goat human antibody complement C3 $F(ab)_2$ fragment (Cappel) as the capture antibody and peroxidase-conjugated goat IgG fraction to human complement C3 (Cappel) as the detection antibody. For comparison, human serum and C57BL/6 serum were used as positive and negative controls, respectively. For quantification of total serum IgM and IgG in humanized mice, the Bethyl Human IgM ELISA Quantitation Kit and the Human IgG ELISA Quantitation Kit (Biomol) were used according to the manufacturer's instructions. Optical density was measured with a VersaMax tunable microplate reader (Molecular Devices) at 450 and 650 nm.

Isolation of Genomic DNA and Genotyping

Human FcγRIIA-131H/R and FcγRIIIA-158F/V polymorphisms were determined as previously described (Baerenwaldt et al., 2011). In brief, 250 μl of umbilical cord blood samples was taken and stored at −20°C before HSCs were isolated. Genomic DNA was isolated with the QiaAmp DSP Blood Mini Kit (QIAGEN) following the instructions of the distributor. To identify the

FcγRIIA-131H/R and FcγRIIIA-158F/V allelic variants, allele-specific nested PCRs were performed as previously described (Baerenwaldt et al., 2011).

Osteoclast Differentiation

Total single-cell bone marrow preparations of humanized Rag2/γc/FcRγ−/− mice or human peripheral blood (after red blood cell lysis) were cultured overnight with 30 ng/ml of human M-CSF. For osteoclast differentiation, the nonadherent cells were cultured further in α-MEM supplemented with 10% heat-inactivated fetal calf serum, glutamine, penicillin, and streptomycin (all from Invitrogen); 30 ng/ml human M-CSF; and 50 ng/ml hRANKL (PeproTech). After 14 days of culture, the cells were stained for TRAP by using Leukocyte Acid Phosphatase Kit 386A (Sigma-Aldrich) to identify osteoclasts. To determine osteoclast activity, the OsteoLyse Assay Kit (Lonza) was used according to the manufacturer's instructions. In brief, 100,000 nonadherent cells were seeded and after 7 days under osteoclast differentiation conditions, the supernatant was collected. The released fluorescence in the medium was measured using a time-resolved fluorescence fluorimeter (Wallac Victor3; PerkinElmer).

Statistics

The statistical significance of the data was determined as indicated in the figure legends. In brief, the Mann-Whitney test or Wilcoxon signed rank test was applied to compare two experimental groups, and the Kruskal-Wallis test or ANOVA (and subsequent post hoc tests or Mann-Whitney test and Bonferroni correction) were used to determine statistical differences between more than two groups. To indicate different levels of significance, a p value of 0.05 was assigned one asterisk, and a value smaller than 0.05 but larger than 0.001 was assigned two asterisks.

SUPPLEMENTAL INFORMATION

Supplemental Information includes three figures and three tables and can be found with this article online at http://dx.doi.org/10.1016/j.celrep.2014.02.041.

AUTHOR CONTRIBUTIONS

F.N. led the research team, designed the experiments, and wrote the paper. A.L., A.B., M.S., B.L., and I.S. designed and performed experiments. A.M., N.M., A.H., G.H., R.R., and D.D. provided essential materials, analyzed experiments, and provided direction and guidance for the design of the experiments.

ACKNOWLEDGMENTS

We thank Jeffrey Ravetch (Rockefeller University, New York), Mark Hogarth (Burnet Institute), and Hergen Spits (Academisch Medisch Center) for mice and Jeffrey Stavenhagen (Macrogenics) for the 2B6 antibody. We are grateful to the Placenta Blood Bank at the University of Erlangen and the Klinikum Fürth for providing umbilical cord blood samples and to Heike Albert, Heike Danzer, Melissa Woigk, and Monique Hoffmann for expert technical assistance. This study was supported by grants from the DFG-SFB643 (F.N. and D.D.), the Bavarian Genome Research Network (F.N. and D.D.), and the DFG Emmy Noether Program (D.D.).

Received: July 11, 2013
Revised: October 27, 2013
Accepted: February 27, 2014
Published: March 27, 2014

REFERENCES

Baerenwaldt, A., Lux, A., Danzer, H., Spriewald, B.M., Ullrich, E., Heidkamp, G., Dudziak, D., and Nimmerjahn, F. (2011). Fcγ receptor IIB (FcγRIIB) maintains humoral tolerance in the human immune system in vivo. Proc. Natl. Acad. Sci. USA *108*, 18772–18777.

Baudino, L., Nimmerjahn, F., Azeredo da Silveira, S., Martinez-Soria, E., Saito, T., Carroll, M., Ravetch, J.V., Verbeek, J.S., and Izui, S. (2008). Differential contribution of three activating IgG Fc receptors (FcgammaRI, FcgammaRIII, and FcgammaRIV) to IgG2a- and IgG2b-induced autoimmune hemolytic anemia in mice. J. Immunol. *180*, 1948–1953.

Beers, S.A., Chan, C.H., James, S., French, R.R., Attfield, K.E., Brennan, C.M., Ahuja, A., Shlomchik, M.J., Cragg, M.S., and Glennie, M.J. (2008). Type II (tositumomab) anti-CD20 monoclonal antibody out performs type I (rituximab-like) reagents in B-cell depletion regardless of complement activation. Blood *112*, 4170–4177.

Beers, S.A., French, R.R., Chan, H.T., Lim, S.H., Jarrett, T.C., Vidal, R.M., Wijayaweera, S.S., Dixon, S.V., Kim, H., Cox, K.L., et al. (2010). Antigenic modulation limits the efficacy of anti-CD20 antibodies: implications for antibody selection. Blood *115*, 5191–5201.

Biburger, M., and Nimmerjahn, F. (2012). Low level of FcγRIII expression on murine natural killer cells. Immunol. Lett. *143*, 53–59.

Biburger, M., Aschermann, S., Schwab, I., Lux, A., Albert, H., Danzer, H., Woigk, M., Dudziak, D., and Nimmerjahn, F. (2011). Monocyte subsets responsible for immunoglobulin G-dependent effector functions in vivo. Immunity *35*, 932–944.

Blom, B., and Spits, H. (2006). Development of human lymphoid cells. Annu. Rev. Immunol. *24*, 287–320.

Bonavida, B. (2007). Rituximab-induced inhibition of antiapoptotic cell survival pathways: implications in chemo/immunoresistance, rituximab unresponsiveness, prognostic and novel therapeutic interventions. Oncogene *26*, 3629–3636.

Bruhns, P., Iannascoli, B., England, P., Mancardi, D.A., Fernandez, N., Jorieux, S., and Daëron, M. (2009). Specificity and affinity of human Fcgamma receptors and their polymorphic variants for human IgG subclasses. Blood *113*, 3716–3725.

Carter, P.J. (2006). Potent antibody therapeutics by design. Nat. Rev. Immunol. *6*, 343–357.

Cartron, G., Dacheux, L., Salles, G., Solal-Celigny, P., Bardos, P., Colombat, P., and Watier, H. (2002). Therapeutic activity of humanized anti-CD20 monoclonal antibody and polymorphism in IgG Fc receptor FcgammaRIIIa gene. Blood *99*, 754–758.

Fossati-Jimack, L., Ioan-Facsinay, A., Reininger, L., Chicheportiche, Y., Watanabe, N., Saito, T., Hofhuis, F.M., Gessner, J.E., Schiller, C., Schmidt, R.E., et al. (2000). Markedly different pathogenicity of four immunoglobulin G isotype-switch variants of an antierythrocyte autoantibody is based on their capacity to interact in vivo with the low-affinity Fcgamma receptor III. J. Exp. Med. *191*, 1293–1302.

Ghia, P., ten Boekel, E., Rolink, A.G., and Melchers, F. (1998). B-cell development: a comparison between mouse and man. Immunol. Today *19*, 480–485.

Goldman, J.P., Blundell, M.P., Lopes, L., Kinnon, C., Di Santo, J.P., and Thrasher, A.J. (1998). Enhanced human cell engraftment in mice deficient in RAG2 and the common cytokine receptor gamma chain. Br. J. Haematol. *103*, 335–342.

Gong, Q., Ou, Q., Ye, S., Lee, W.P., Cornelius, J., Diehl, L., Lin, W.Y., Hu, Z., Lu, Y., Chen, Y., et al. (2005). Importance of cellular microenvironment and circulatory dynamics in B cell immunotherapy. J. Immunol. *174*, 817–826.

Hamaguchi, Y., Uchida, J., Cain, D.W., Venturi, G.M., Poe, J.C., Haas, K.M., and Tedder, T.F. (2005). The peritoneal cavity provides a protective niche for B1 and conventional B lymphocytes during anti-CD20 immunotherapy in mice. J. Immunol. *174*, 4389–4399.

Hamaguchi, Y., Xiu, Y., Komura, K., Nimmerjahn, F., and Tedder, T.F. (2006). Antibody isotype-specific engagement of Fcgamma receptors regulates B lymphocyte depletion during CD20 immunotherapy. J. Exp. Med. *203*, 743–753.

Hirano, M., Davis, R.S., Fine, W.D., Nakamura, S., Shimizu, K., Yagi, H., Kato, K., Stephan, R.P., and Cooper, M.D. (2007). IgEb immune complexes activate macrophages through FcgammaRIV binding. Nat. Immunol. *8*, 762–771.

Hogarth, P.M. (2002). Fc receptors are major mediators of antibody based inflammation in autoimmunity. Curr. Opin. Immunol. *14*, 798–802.

Ito, M., Hiramatsu, H., Kobayashi, K., Suzue, K., Kawahata, M., Hioki, K., Ueyama, Y., Koyanagi, Y., Sugamura, K., Tsuji, K., et al. (2002). NOD/SCID/gamma(c)(null) mouse: an excellent recipient mouse model for engraftment of human cells. Blood *100*, 3175–3182.

Johnson, T.A., and Press, O.W. (2000). Therapy of B-cell lymphomas with monoclonal antibodies and radioimmunoconjugates: the Seattle experience. Ann. Hematol. *79*, 175–182.

Kaneko, Y., Nimmerjahn, F., Madaio, M.P., and Ravetch, J.V. (2006). Pathology and protection in nephrotoxic nephritis is determined by selective engagement of specific Fc receptors. J. Exp. Med. *203*, 789–797.

Kasperkiewicz, M., Nimmerjahn, F., Wende, S., Hirose, M., Iwata, H., Jonkman, M.F., Samavedam, U., Gupta, Y., Möller, S., Rentz, E., et al. (2012). Genetic identification and functional validation of FcγRIV as key molecule in autoantibody-induced tissue injury. J. Pathol. *228*, 8–19.

Legrand, N., Weijer, K., and Spits, H. (2008). Experimental model for the study of the human immune system: production and monitoring of "human immune system" Rag2-/-gamma c-/- mice. Methods Mol. Biol. *415*, 65–82.

Legrand, N., Ploss, A., Balling, R., Becker, P.D., Borsotti, C., Brezillon, N., Debarry, J., de Jong, Y., Deng, H., Di Santo, J.P., et al. (2009). Humanized mice for modeling human infectious disease: challenges, progress, and outlook. Cell Host Microbe *6*, 5–9.

Li, Y., Chen, Q., Zheng, D., Yin, L., Chionh, Y.H., Wong, L.H., Tan, S.Q., Tan, T.C., Chan, J.K., Alonso, S., et al. (2013). Induction of functional human macrophages from bone marrow promonocytes by M-CSF in humanized mice. J. Immunol. *191*, 3192–3199.

Lux, A., and Nimmerjahn, F. (2011). Impact of differential glycosylation on IgG activity. Adv. Exp. Med. Biol. *780*, 113–124.

Lux, A., and Nimmerjahn, F. (2013). Of mice and men: the need for humanized mouse models to study human IgG activity in vivo. J. Clin. Immunol. *33* (*Suppl 1*), S4–S8.

Lux, A., Yu, X., Scanlan, C.N., and Nimmerjahn, F. (2013). Impact of immune complex size and glycosylation on IgG binding to human FcγRs. J. Immunol. *190*, 4315–4323.

Mancardi, D.A., Iannascoli, B., Hoos, S., England, P., Daëron, M., and Bruhns, P. (2008). FcgammaRIV is a mouse IgE receptor that resembles macrophage FcepsilonRI in humans and promotes IgE-induced lung inflammation. J. Clin. Invest. *118*, 3738–3750.

Mancardi, D.A., Jönsson, F., Iannascoli, B., Khun, H., Van Rooijen, N., Huerre, M., Daëron, M., and Bruhns, P. (2011). Cutting Edge: The murine high-affinity IgG receptor FcγRIV is sufficient for autoantibody-induced arthritis. J. Immunol. *186*, 1899–1903.

Montalvao, F., Garcia, Z., Celli, S., Breart, B., Deguine, J., Van Rooijen, N., and Bousso, P. (2013). The mechanism of anti-CD20-mediated B cell depletion revealed by intravital imaging. J. Clin. Invest. *123*, 5098–5103.

Musolino, A., Naldi, N., Bortesi, B., Pezzuolo, D., Capelletti, M., Missale, G., Laccabue, D., Zerbini, A., Camisa, R., Bisagni, G., et al. (2008). Immunoglobulin G fragment C receptor polymorphisms and clinical efficacy of trastuzumab-based therapy in patients with HER-2/neu-positive metastatic breast cancer. J. Clin. Oncol. *26*, 1789–1796.

Nakashima, T., Hayashi, M., and Takayanagi, H. (2012). New insights into osteoclastogenic signaling mechanisms. Trends Endocrinol. Metab. *23*, 582–590.

Nimmerjahn, F., and Ravetch, J.V. (2005). Divergent immunoglobulin g subclass activity through selective Fc receptor binding. Science *310*, 1510–1512.

Nimmerjahn, F., and Ravetch, J.V. (2008). Fcgamma receptors as regulators of immune responses. Nat. Rev. Immunol. *8*, 34–47.

Nimmerjahn, F., Bruhns, P., Horiuchi, K., and Ravetch, J.V. (2005). FcgammaRIV: a novel FcR with distinct IgG subclass specificity. Immunity *23*, 41–51.

Nimmerjahn, F., Lux, A., Albert, H., Woigk, M., Lehmann, C., Dudziak, D., Smith, P., and Ravetch, J.V. (2010). FcγRIV deletion reveals its central role for IgG2a and IgG2b activity in vivo. Proc. Natl. Acad. Sci. USA *107*, 19396–19401.

Otten, M.A., van der Bij, G.J., Verbeek, S.J., Nimmerjahn, F., Ravetch, J.V., Beelen, R.H., van de Winkel, J.G., and van Egmond, M. (2008). Experimental antibody therapy of liver metastases reveals functional redundancy between Fc gammaRI and Fc gammaRIV. J. Immunol. *181*, 6829–6836.

Ravetch, J.V., and Nimmerjahn, F. (2008). Fc receptors. In Fundamental Immunology, Fifth Edition, W.E. Paul, ed. (Philadelphia: Lippincott-Raven).

Sanz, I., and Lee, F.E. (2010). B cells as therapeutic targets in SLE. Nat Rev Rheumatol *6*, 326–337.

Sanz, I., Anolik, J.H., and Looney, R.J. (2007). B cell depletion therapy in autoimmune diseases. Front. Biosci. *12*, 2546–2567.

Seeling, M., Hillenhoff, U., David, J.P., Schett, G., Tuckermann, J., Lux, A., and Nimmerjahn, F. (2013). Inflammatory monocytes and Fcγ receptor IV on osteoclasts are critical for bone destruction during inflammatory arthritis in mice. Proc. Natl. Acad. Sci. USA *110*, 10729–10734.

Shan, D., Ledbetter, J.A., and Press, O.W. (1998). Apoptosis of malignant human B cells by ligation of CD20 with monoclonal antibodies. Blood *91*, 1644–1652.

Shultz, L.D., Brehm, M.A., Garcia-Martinez, J.V., and Greiner, D.L. (2012). Humanized mice for immune system investigation: progress, promise and challenges. Nat. Rev. Immunol. *12*, 786–798.

Smith, K.G., and Clatworthy, M.R. (2010). FcgammaRIIB in autoimmunity and infection: evolutionary and therapeutic implications. Nat. Rev. Immunol. *10*, 328–343.

Smith, P., DiLillo, D.J., Bournazos, S., Li, F., and Ravetch, J.V. (2012). Mouse model recapitulating human Fcγ receptor structural and functional diversity. Proc. Natl. Acad. Sci. USA *109*, 6181–6186.

St Clair, E.W. (2009). Novel targeted therapies for autoimmunity. Curr. Opin. Immunol. *21*, 648–657.

Syed, S.N., Konrad, S., Wiege, K., Nieswandt, B., Nimmerjahn, F., Schmidt, R.E., and Gessner, J.E. (2009). Both FcgammaRIV and FcgammaRIII are essential receptors mediating type II and type III autoimmune responses via FcRgamma-LAT-dependent generation of C5a. Eur. J. Immunol. *39*, 3343–3356.

Takai, T. (2002). Roles of Fc receptors in autoimmunity. Nat. Rev. Immunol. *2*, 580–592.

Tanaka, S., Saito, Y., Kunisawa, J., Kurashima, Y., Wake, T., Suzuki, N., Shultz, L.D., Kiyono, H., and Ishikawa, F. (2012). Development of mature and functional human myeloid subsets in hematopoietic stem cell-engrafted NOD/SCID/IL2rγKO mice. J. Immunol. *188*, 6145–6155.

Traggiai, E., Chicha, L., Mazzucchelli, L., Bronz, L., Piffaretti, J.C., Lanzavecchia, A., and Manz, M.G. (2004). Development of a human adaptive immune system in cord blood cell-transplanted mice. Science *304*, 104–107.

Uchida, J., Hamaguchi, Y., Oliver, J.A., Ravetch, J.V., Poe, J.C., Haas, K.M., and Tedder, T.F. (2004a). The innate mononuclear phagocyte network depletes B lymphocytes through Fc receptor-dependent mechanisms during anti-CD20 antibody immunotherapy. J. Exp. Med. *199*, 1659–1669.

Uchida, J., Lee, Y., Hasegawa, M., Liang, Y., Bradney, A., Oliver, J.A., Bowen, K., Steeber, D.A., Haas, K.M., Poe, J.C., and Tedder, T.F. (2004b). Mouse CD20 expression and function. Int. Immunol. *16*, 119–129.

van der Bij, G.J., Bögels, M., Otten, M.A., Oosterling, S.J., Kuppen, P.J., Meijer, S., Beelen, R.H., and van Egmond, M. (2010). Experimentally induced liver metastases from colorectal cancer can be prevented by mononuclear phagocyte-mediated monoclonal antibody therapy. J. Hepatol. *53*, 677–685.

Waldmann, T.A. (2003). Immunotherapy: past, present and future. Nat. Med. *9*, 269–277.

Weiner, L.M., Surana, R., and Wang, S. (2010). Monoclonal antibodies: versatile platforms for cancer immunotherapy. Nat. Rev. Immunol. *10*, 317–327.

Weng, W.K., and Levy, R. (2003). Two immunoglobulin G fragment C receptor polymorphisms independently predict response to rituximab in patients with follicular lymphoma. J. Clin. Oncol. *21*, 3940–3947.

Weng, W.K., Czerwinski, D., Timmerman, J., Hsu, F.J., and Levy, R. (2004). Clinical outcome of lymphoma patients after idiotype vaccination is correlated with humoral immune response and immunoglobulin G Fc receptor genotype. J. Clin. Oncol. *22*, 4717–4724.

Yazawa, N., Hamaguchi, Y., Poe, J.C., and Tedder, T.F. (2005). Immunotherapy using unconjugated CD19 monoclonal antibodies in animal models for B lymphocyte malignancies and autoimmune disease. Proc. Natl. Acad. Sci. USA *102*, 15178–15183.